Electromechanical-induced antiferroelectric–ferroelectric phase transition in $PbLa(Zr,Sn,Ti)O_3$ ceramic*

Zhang Chong-Hui(张崇辉)[a)b)†], Xu Zhuo(徐 卓)[b)], Gao Jun-Jie(高俊杰)[b)], Zhu Chang-Jun(朱长军)[a)], and Yao Xi(姚 熹)[b)]

[a)] *School of Science, Xi'an Polytechnic University, Xi'an* 710048, *China*

[b)] *Electronic Materials Research Laboratory, Key Laboratory of the Ministry of Education, Xi'an Jiaotong University, Xi'an* 710048, *China*

(Received 25 October 2010; revised manuscript received 9 April 2011)

Antiferroelectric–ferroelectric (AFE–FE) phase transition in ceramic $Pb_{0.97}La_{0.02}(Zr_{0.75}Sn_{0.136}Ti_{0.114})O_3$ (PLZST) was studied by dielectric spectroscopy as functions of frequency (10^2–10^5 Hz) and pressure (0–500 MPa) under a DC electric field. The hydrostatic pressure-dependent remnant polarization and dielectric constant were measured. The results show that remnant polarization of the metastable rhombohedral ferroelectric PLZST poled ceramic decreases sharply and depoles completely at phase transition under hydrostatic pressure. The dielectric constant undergoes an abrupt jump twice during a load and unload cycle under an electric field. The two abrupt jumps correspond to two phase transitions, FE–AFE and AFE–FE.

Keywords: antiferroelectric ceramic, dielectric constant, hydrostatic pressure, phase transition

PACS: 77.80.–e, 77.22.Ch, 62.50.–p **DOI:** 10.1088/1674-1056/20/9/097702

1. Introduction

The perovskites $PbZrO_3$ and $PbTiO_3$ form a continuous series of solid solutions of the formula $PbZr_{1-x}Ti_xO_3$ over the whole composition range. The solid solutions, commonly referred to as PZT, have a lot of excellent characteristics and detailed research has been conducted to date.[1−6] Research has revealed that in a lanthanum doped A-site modified $Pb(Zr,Sn,Ti)O_3$ (PZST) system, a variety of ferroelectric and nonferroelectric transitions can be induced by variations in composition, temperature, electric-field or pressure.[7−9] They also exhibit large spontaneous polarizations and piezoelectric coefficients. Utilizing their special characteristics, various ferroelectric devices can be fabricated, for instance, actuators with large electric-induced strain, micro-mechanic clamps with shape memory, energy converters with pressure-induced releasing bound charge in a short time, and ultra-high-density energy storage with a nonlinear double polarization–electric field loop.

Most previous research on the Pb(Zr, Sn, Ti) (PZST) system was focused on fabrication methods and the influence of temperature or electric-field on the properties of PZST systems. Pressure, however, is another important external field which affects the characteristics of PZST systems, and can induce more interesting properties. Samara *et al.* studied hydrostatic pressure-induced relaxation and phase transition in several ferroelectric ceramics or single crystals.[10−12] Our previous work investigated the phase transition of hydrostatic pressure-induced ferroelectric (FE)–antiferroelectric (AFE) ceramics.[13−15] AFE lead lanthanum zirconate titanate stannate (PLZST) near the morphotropic phase boundary (MPB) of PLZST diagram switches to a FE phase with the application of electric field and sustains in a metastable FE state. The poled FE PLZST ceramic can return to AFE when it is depoled through heat treatment. In addition to the heat treatment, hydrostatic pressure can also cause poled PLZST to return to the AFE state. In this paper, a compound ceramic with the chemical composition $Pb_{0.97}La_{0.02}(Zr_{0.75}Sn_{0.136}Ti_{0.114})O_3$ (PLZST) was prepared by a traditional solid-state reaction process. The sample was near the FE–AFE phase bound-

*Project supported by the National Basic Research Program of China (Grant No. 2009CB623306), the International Science & Technology Cooperation Program of China (Grant No. 2010DFR50480), and the National Natural Science Foundation of China (Grant No. 10976022).

†Corresponding author. E-mail: zhchh226gch@126.com

© 2011 Chinese Physical Society and IOP Publishing Ltd

ary in the PLZST diagram. The relationship between remnant polarization and hydrostatic pressure was studied and, the FE–AFE phase transition induced by the DC bias field and hydrostatic pressure was investigated by measuring the dielectric properties as functions of pressure, frequency and electric field.

2. Experimental procedure

A ceramic with the chemical composition $Pb_{0.97}La_{0.02}(Zr_{0.75}Sn_{0.136}Ti_{0.114})O_3$ was selected as the sample, which was fabricated by a traditional solid-state reaction process of oxides. The composition was close to the FE/AFE phase boundary and located on the antiferroelectric side. Reagent-grade oxide powders of La_2O_3, PbO, ZrO_2, SnO and TiO_2 were used as raw materials and commixed according to the given composition with an addition of 2 mol% excess PbO to compensate for losses. The mixtures were calcined at 850°C for 4 h to obtain the perovskite structure. The calcined powders with added 2 wt% PVA (polyvinyl alcohol) were cold pressed into poles, 12 mm in diameter, under a pressure of 170 MPa. The poles were sintered in a lead-compensating atmosphere for 2 h at 1240°C. The ceramic poles were cut into circle flakes of 0.7 mm in thickness and both faces of the specimens were entirely covered with silver to serve as electrodes. The ferroelectric hysteresis loop was measured at room temperature using a ferroelectric tester (TF ANALYZER2000, aixACT Inc, German). The piezoelectric constant d_{33} was measured using a quasistatic piezo-d_{33} meter (Institute of Acoustics, Chinese Academy of Sciences, ZJ-3A). The dielectric properties of the specimen were studied as a function of hydrostatic pressure (0–500 MPa) and frequency (10^2–10^5 Hz) under different DC bias field (0–12 $kV \cdot cm^{-1}$) using a HP4274A LCR meter connected to a computer automatic measurement system. The hydrostatic pressure system consisted of a conventional high pressure apparatus (3×10^5 kg two directions load) and high-pressure vessel. The benzoline and aero kerosene 30/70 (V/V) mixture was employed as pressure transmitting media. The pressure equipment was described in Ref. [16]. The pressure was measured by the change in resistance of a calibrated manganin coil, which was detected using a digital multi-meter (Keithley 2000) connected to the computer and the error was less than ±2%. The applied DC bias was supplied by a high voltage DC power (Mode PS350/5000V-25W, USA).

3. Results and discussion

3.1. The hydrostatic pressure dependence of remnant polarization

The polarization–electric field (P–E) hysteresis loop of the original sample at room temperature is illustrated in Fig. 1(a). It can be seen from the first loop (dashed line O–A–B) of the fresh PLZST sample that the AFE to FE switching field E_{AF} is about 10 $kV \cdot cm^{-1}$. However, the coercive field (E_c) is 7.53 $kV \cdot cm^{-1}$ and the maximum remnant polarization is about 29.7 $\mu C \cdot cm^{-2}$. The E_{AF} is larger than the E_c, which is very characteristic of AFE ceramic behaviour. The electric-induced AFE–FE phase transition was observed at E_{AF}. It was not able to return to the antiferroelectric state when the electric field was removed. The sample was in an electric field-induced metastable FE state and the piezoelectric coefficients d_{33} was 96 $pC \cdot N^{-1}$. The relative dielectric constant-temperature spectrum (ε'–T) of the poled sample shows that two phase transitions take place, separately, during heating process from room temperature to 300°C (see Fig. 1(b)). The first one is an EF–AFE phase transition at 98°C and the second is the transition from AFE to paraelectric (AFE–PE) at 167°C.

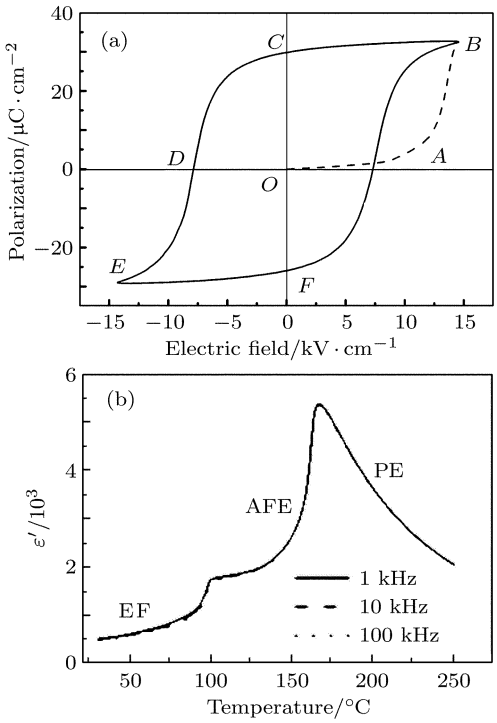


Fig. 1. (a) Polarization–electric field hysteresis loop and (b) the relative dielectric constant-temperature spectrum of PLZST. The coercive field (E_c) is 7.53 $kV \cdot cm^{-1}$, and the maximum remnant polarization is 29.7 $\mu C \cdot cm^{-2}$.

Because the PLZST ceramic sample is located in the AFE region near the boundary between the antiferroelectric tetragonal (A_T) and the ferroelectric rhombohedral (F_R) phases, it switches into the metastable rhombohedral ferroelectric state after being poled at a DC electric field of 20 kV$\cdot$ cm^{-1}. The P–E loop is close to one of the typical ferroelectric materials after the first cycle. The pressure-induced phase transition from the ferroelectric rhombohedral phase to the antiferroelectric tetragonal phase was observed previously at a certain hydrostatic pressure,[13] the corresponding pressure, referred to as phase transition pressure or quasi Cure pressure, is denoted by P_c. The bounded charge was released in a short time at P_c. Through releasing the charge collected by a big capacitance (15 pF), the remnant polarization P_r was obtained. Figure 2 shows the curves of remnant polarization (closed symbols) versus hydrostatic pressure. The insert is the curve of pressure versus time and the average rate of pressure increase is 8.8 MPa$\cdot$s^{-1}. It can be seen from Fig. 2 that the P_r curve decreases sharply and the bounded charge is completely released simultaneously. The sample returns to the tetragonal antiferroelectric phase. The remnant polarization varies from 29.7 μC $\cdot$cm^{-2} to 0 at P_c in the process. The remnant polarization has "on/off" characteristics when hydrostatic pressure increases continuously. The sample exhibits characteristics of continuous pressure-induced phase transition. The sample undergoes FE–AFE phase transition under hydrostatic pressure because d_{33} decreases to 0 and the dielectric constants recover to their original values for different frequencies. Additionally, the phase transition is a second transition, which is in the pressure range of 156–239 MPa.

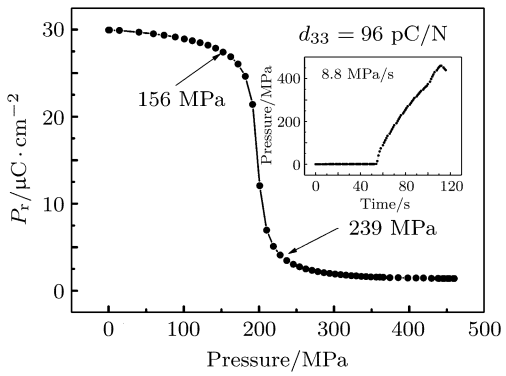


Fig. 2. Curves of remnant polarization of poled PLZST versus hydrostatic pressure. The insert is pressure–time curve, the average load rate is 8.8 MPa$\cdot$s^{-1}.

3.2. The hydrostatic pressure dependence of the dielectric constant under DC bias

The hydrostatic pressure dependence of the poled sample dielectric constant at four frequencies (0.4, 1, 10 and 100 kHz) in loaded and unloaded processes is shown in Fig. 3(a). The pressure was adjustable in steps of approximately 30 MPa. The dielectric constant was measured stepwise at different pressures, both increasing pressure and decreasing pressure processes were used for approximately 1.5 h. To ensure the pressure balance of liquid transmitting media in the high pressure cavity, it was necessary to wait 60 s after each load or unload process. It can be seen from Fig. 3 that the curves change sharply at a certain pressure, the corresponding pressure agrees well with phase transition pressure (P_c) obtained from the P_r–pressure curve (see Fig. 2). The P_c is 186 MPa and the dielectric constant varies from about 500 to 860, and the P_c is independent of frequency. In the pressure increasing process, the dielectric constant increases slowly with increasing pressure when the pressure is less than P_c. Once the pressure is larger than P_c, the dielectric constant decreases slowly with increasing pressure. As there is a pressure-induced phase transition from FE to AFE at P_c, the sample is in FE state when the pressure is less than P_c and it changes back to AFE when the pressure is higher than P_c, up to 550 MPa. The dielectric constant increases slowly with decreasing pressure in the subsequent unload process. There is no evidence in the dielectric constant for a reverse transition to the FE phase during the pressure release without DC bias. Once in the A_T phase, the sample exhibits a small hysteresis on lowering pressure. The change of micro-structure inside the sample was reflected in the variety of sample dielectric properties.[10,13]

The dielectric properties as functions of hydrostatic pressure and frequency under different applied DC positive biases were studied at room temperature in both pressure increasing and pressure decreasing processes. When the DC positive bias, E = 12 kV$\cdot$cm^{-1}, was applied, the dielectric behaviour as a function of hydrostatic pressure was similar to that at above zero DC bias (see Fig. 3(a)). However, the phase transition P_c of FE–AFE increases to 283 MPa as shown in Fig. 3(b). In addition to the sharp change of the dielectric constant at 283 MPa, there is a rapid drop of ε' at 100 MPa during the lowering pressure process (see Fig. 3(b)).

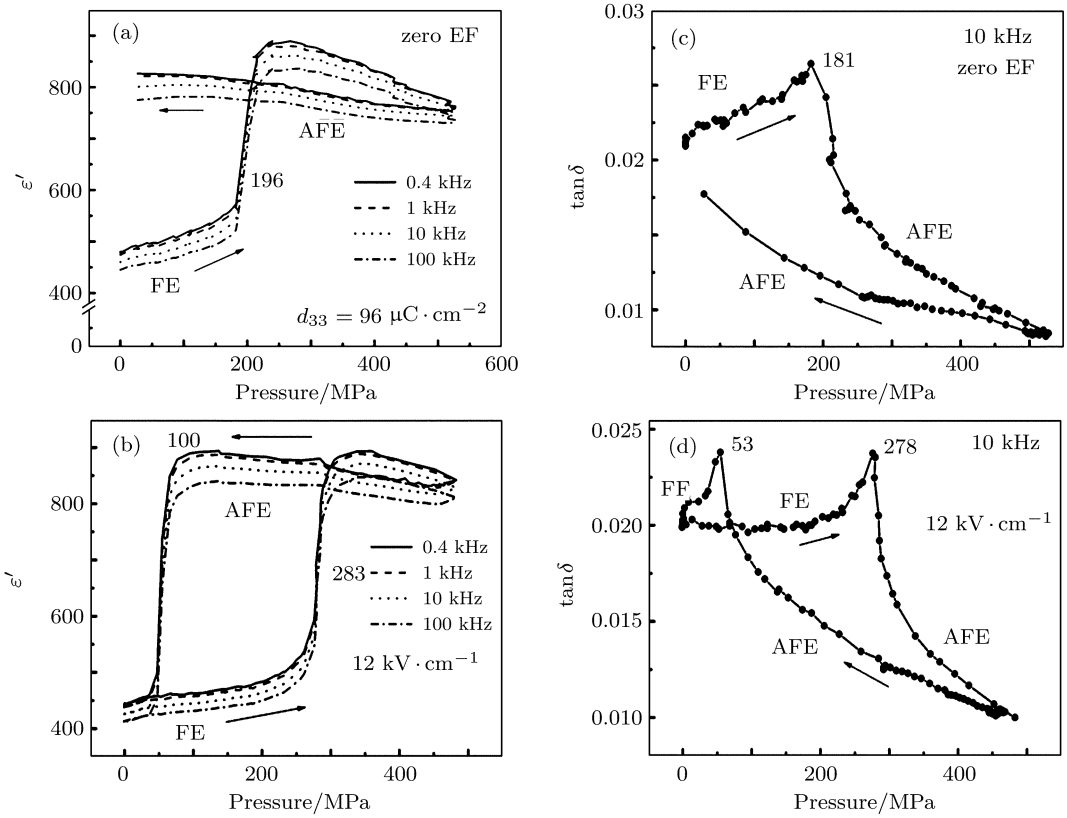


Fig. 3. Hydrostatic pressure dependence of dielectric constant ((a), (b)) and dielectric loss ((c), (d)) under various DC electric fields. The arrows denote the pressure increasing and decreasing processes. (a), (c) without electric field; (b), (d) with electric field of 12 kV/cm.

The two dielectric jumps correspond to the two phase transitions. The first is the pressure-induced phase transition from the FE state to the AFE state during increasing pressure. The second is the electric field-induced phase transition from AFE to FE during decreasing pressure. The sample returns to the FE state for a DC bias higher than $E_{\rm AF}$ (10 kV · cm^{-1}). The d_{33} of the sample recovers to 96 pC · N^{-1} again. There are two peaks at 278 MPa and 53 MPa on the dielectric loss-pressure curves (tan δ–P) for 10 kHz as shown in Fig. 3(d). The peak at 278 MPa corresponds to the FE–AFE phase transition. The peak at 53 MPa corresponds to the AFE–FE phase transition. The peak pressures are lower than the abrupt change pressure of the dielectric constant. The sample exhibits a small hysteresis at the AFE state on increasing pressure and decreasing pressure. The ε'-P loop forms when a higher bias larger than 10 kV · cm^{-1} is applied.

Research on partial FE micro-domain distribution in the AFE body in random orientations has been conducted previously.[17] At first, the AFE domain and FE domain were oriented along the electric field direction to minimize free energy when a sample was exposed to a low electric field. The FE micro-domains grow into electric domain nuclei in the AFE body with increasing electric field. Once the applied electric field is large enough, the electric domain nuclei amalgamate into the FE macro-domain, at the same time, the FE macro-domain continually grows and impenetrates the whole sample to realize the AFE–FE transition. This process is accompanied by a distinct volume increase.[18–20] Tha electric field promotes cell volume enlargement. However, hydrostatic pressure increases free energy and mechanical stress to suppress domain reorientation along the electric field direction and FE domain growth, namely, hydrostatic pressure, hinders the increase of cell volume. Both the force of the electric field and the hydrostatic pressure have effects on sample properties simultaneously. The electric field acts as a long-range force and hydrostatic pressure as a short-range force. The Coulomb force varies with inter-ionic distance, as $1/r^2$, whereas the short-range force varies as $1/r^n$, where n has a large value. Thus, for a given increase in pressure, the correlation length decreases much more rapidly than the growth of the ferroelectric macro-domain. Consequently, the AFE–FE phase transition is determined by the competition between the electric field force and pressure.

4. Conclusion

The phase transition properties were obtained from dielectric constant and remnant polarization measurements. The sample was switched from antiferroelectric to metastable ferroelectric after being poled and the poled ceramic underwent an FE–AFE phase transition at low hydrostatic pressure at room temperature. The sample undergoes two phase transitions, FE–AFE and AFE–FE, during increasing pressure and subsequent decreasing pressure respectively. The dielectric properties change rapidly at the point of phase transition induced by the DC electric field. Hydrostatic pressure favours the stability of the smaller-volume antiferroelectric phase; in contrast, the DC electric field favours the ferroelectric phase. The above results provide valuable data for the better understanding of phase transition mechanisms under external electric fields, pressures, and temperatures.

References

[1] Rouquette J, Haines J, Bornand V, Pintard M, Papet Ph, Bonnet B and Gorelli F A 2003 *Solid State Sci.* **5** 451

[2] Garg A and Goel T C 1999 *Mat. Sci. Eng.* B **60** 128

[3] Kong L B and Ma J 2001 *Mater. Lett.* **51** 95

[4] Cereceda N, Noheda B, Fdez-del-Castillo J R, Gonzalo J A, de Frutos J and González A M 1999 *J. Eur. Ceram. Soc.* **19** 1259

[5] Soares M R, Senos A M R and Mantas P Q 2000 *J. Eur. Ceram. Soc.* **20** 321

[6] Berlincourt D 1966 *IEEE Trans. Sonics Ultrason* **SU-13** 116

[7] Shirane G and Suauki K 1952 *J. Phys. Soc. Jpn.* **8** 7333

[8] Xue L H, Li Q, Zhang Y L, Zhen X H, Liu R and Wang L 2006 *Mat. Sci. Eng.* B **132** 253

[9] Liu P and Yao X 2004 *Solid State Commun.* **132** 809

[10] Avdeev M, Jorgensen J D, Short S, Samara G A, Venturini E L, Yang P and Morosin B 2006 *Phys. Rev.* B **73** 064105

[11] Samara G A 1998 *J. Appl. Phys.* **84** 2538

[12] Samara G A and Venturini E L 2001 *Phys. Rev.* B **63** 184104

[13] Xu Z, Feng Y J, Zheng S G, Jin A, Wang F L and Yao X 2001 *Acta Phys. Sin.* **50** 1787 (in Chinese)

[14] Xu Z, Feng Y J, Zheng S G, Jin A, Wang F L and Yao X 2003 *Mat. Sci. Eng.* B **99** 441

[15] Dai Z H, Yao X and Xu Z 2009 *Acta Phys. Sin.* **58** 3520 (in Chinese)

[16] Zhang C H, Xu Z, Gao J J and Yao X 2010 *High Pressure Research* **30** 473

[17] Feng Y J, Xu Z, Wei X Y and Yao X 2003 *Acta Phys. Sin.* **52** 1255 (in Chinese)

[18] Park S E, Pan M J, Markowski K, Yoshikawa S and Cross L E 1997 *J. Appl. Phys.* **82** 1798

[19] Shebanov L, Kusnetsov M and Sternberg A 1994 *J. Appl. Phys.* **76** 4301

[20] Blue C T, Hicks J C, Park S E, Yoshikawa S and Cross L E 1996 *Appl. Phys. Lett.* **68** 2942